https://doi.org/10.5194/acp-2021-742
Preprint. Discussion started: 9 September 2021

Atmospheric Chemistry and Physics Discussions

Emission factors of long-lived volatile organic compounds from the 2019-2020 Australian wildfires during the COALA campaign

Asher P. Mouat[1], Clare Paton-Walsh[3], Jack B. Simmons[3], Jhonathan Ramirez-Gamboa[3], David W. T. Griffith[3] and Jennifer Kaiser[1,2]

[1]Department of Civil and Environmental Engineering, Georgia Institute of Technology, Atlanta GA 30332, USA

[2]Department of Earth and Atmospheric Sciences, Georgia Institute of Technology, Atlanta GA 30332, USA

[3]School of Earth, Atmospheric, and Life Sciences, University of Wollongong, Wollongong, NSW, Australia 2522

Correspondence to: Asher Mouat (amouat3@gatech.edu)

Abstract. In 2019/2020, Australia experienced its largest wildfire season on record. Smoke covered hundreds of square kilometers across the southeastern coast and reached the site of the 2020 COALA (**C**haracterizing **O**rganics and **A**erosol **L**oading over **A**ustralia) field campaign in New South Wales. Using a subset of nighttime observations made by a proton-transfer-reaction time-of-flight mass spectrometer (PTR-ToF-MS), we calculate emission ratios (ERs) and factors (EFs) for 21 volatile organic compounds (VOCs). We restrict our analysis to VOCs with sufficiently high lifetimes to be minimally impacted by oxidation over the ~8 h between when the smoke was emitted and when it arrived at the field site. We use oxidized VOC to VOC ratios to assess the total amount of radical oxidation: maleic anhydride/furan to assess OH oxidation, and (cis-2-butenediol + furanone)/furan to assess NO_3 oxidation. We compare ERs calculated from the freshest portion of the plume to ERs calculated using the entire nighttime period. Finding good agreement between the two, we are able to extend our analysis to VOCs measured in more chemically aged portions of the plume. Our analysis provides ERs and EFs for 9 compounds not previously reported for temperate forests in Australia: acrolein, pentanones/methylbutanal, methyl propanoate, methyl methacrylate, propene, maleic anhydride, benzaldehyde, methyl guaiacol, and methylbenzoic acid. We compare our results with two studies in similar Australian biomes, and two studies focused on US temperate forests. We find mixed agreement for EFs presented from previous studies of Australian wildfires, and generally good agreement with studies focused on fires in the Western US. This suggests that comprehensive field measurements of biomass burning VOC emissions in other regions may be applicable to Australian temperate forests.

1 Introduction

Wildfire smoke significantly affects atmospheric composition, chemistry, human health, and radiative balance (Akagi et al., 2011). Wildfire season duration and intensity are predicted to increase in the future, suggesting a growing influence of biomass burning in coming decades (Liu et al., 2010). Volatile organic compounds (VOCs) emitted from biomass burning (BBVOCs) are directly harmful to human health and can contribute to the formation of ozone and secondary organic aerosol (SOA) (Akagi et al., 2012; Keywood et al., 2013; Lawson et al., 2015; Sekimoto et al., 2017). Predictions of BBVOC emissions are complicated by the complexity of combustion and fuel characteristics, and model parametrizations are based on a limited number of field observations (Hatch et al., 2015; Sekimoto et al., 2018).

Australia wildfires emit 7-8% of global biomass burning emissions, producing more volatilized carbon than the United States and Europe, with smoke plumes significantly influencing local and even global air quality (Ito and Penner, 2004; Keywood et al., 2013; Lawson et al., 2015; Van Der Werf et al., 2010). In 2019/2020, Australia experienced its worst wildfire season on record with an estimated 19 million hectares of land destroyed (Filkov et al., 2020). Despite their impact on atmospheric composition, emissions from Australian wildfires remain poorly constrained in air quality models. Chemistry transport models often use emission factors

https://doi.org/10.5194/acp-2021-742
Preprint. Discussion started: 9 September 2021


Atmospheric Chemistry and Physics Discussions

(EFs, in units of kg VOC emitted/kg fuel burnt) for temperate forests based on measurements in North America (Akagi et al., 2013; Burling et al., 2011), despite differences in fuel type, which is known to influence the speciation of VOCs emitted (Coggon et al., 2016; Hatch et al., 2017; Guérette et al., 2018). Recent studies address a limited number of VOCs emitted from wildfires in Australian forests and savannahs (Paton-Walsh et al., 2014; Lawson et al., 2015; Wang et al., 2017; Guérette et al., 2018). These have shown that EFs of some VOCs (e.g. formic acid, ethane, monoterpenes, acetonitrile) can be 3 – 5 times higher than those in measured in the US.

A complicating factor in deriving EFs from field observations is accounting for the influence of chemical processing. EFs are ideally based on observations close to the fire. When this is not possible, indicators of plume chemical age, such as oxidized VOC (OVOC) to VOC ratios, can be used to diagnose the relative age of a plume. During the day, downwind VOC concentrations are primarily influenced by OH-initiated oxidation. At night, NO_3-initated oxidation can significantly influence observed VOC concentrations (Decker et al., 2019; Kodros et al., 2020). There are several methods in existence for assessing daytime oxidation, but fewer are known for the night (De Gouw et al., 2006; Liu et al., 2016; Gregory et al., 2018; Decker et al., 2019). In this work, we use the maleic anhydride-to-furan ratio introduced in Gkatzelis et al. (2020) to assess OH oxidation. We examine the use of a new OVOC/VOC ratio, cis-2-butenediol+furanone-to-furan, as an indicator of nighttime oxidation.

Here, we use observations from a proton-transfer-reaction time-of-flight mass spectrometer (PTR-ToF-MS) during the 2019-2020 Australian wildfire season to derive emission factors of 21 compounds, including 9 compounds for which there are no previous observations. We examine a subset of smoke-influenced nighttime observations made by a PTR-ToF-MS during the 2020 COALA (**C**haracterizing **O**rganics and **A**erosol **L**oading over **A**ustralia) field campaign. NO_3-initiated oxidation dominated the chemical processing late in the night, as the plume travelled ~8 h to the field site from large, highly active fires to the south. Using co-located PTR-ToF-MS and FTIR measurements of CO_2, CO and CH_4, we derive EFs for 21 longer-lived VOCs ($\tau_{BBVOC+NO3} \geq$ average transport time), 9 of which have not been determined for Australian biomes. We compare these results with five related studies, two focused on Australian temperate forests, two focused on US temperature forests, and one reporting EFs used to represent temperate biomes across the globe. We find generally good agreement across several of these studies and discuss potential reasons for discrepancies seen in EFs for select compounds.

2 Field Site and Instrument Description:

2.1 Field Site and Active Fires

The COALA field site was located in Cataract Scout Park (34.247° S, 150.825° E) at 400 m above sea level, 15 km inland, and 30 km to northwest of the nearest urban area (Wollongong, NSW). Fig. 1 shows the field site relative to the fires active between 1 Feb and 5 Feb 2020. We use the Suomi VIIRS thermal anomalies product filtering for points at high confidence levels to avoid counting any reflective false positives from plains or urban centers. Also plotted is the normalized difference vegetative index (NDVI) which is determined from measurements aboard the MODIS Terra satellite (Didan, 2021). The fires are primarily located in temperate forests along the southeastern coast, with a small inland group near Canberra. These forests consist of open, tall woodlands made up of *Eucalyptus* species grouped generally as dry sclerophyll.

https://doi.org/10.5194/acp-2021-742
Preprint. Discussion started: 9 September 2021

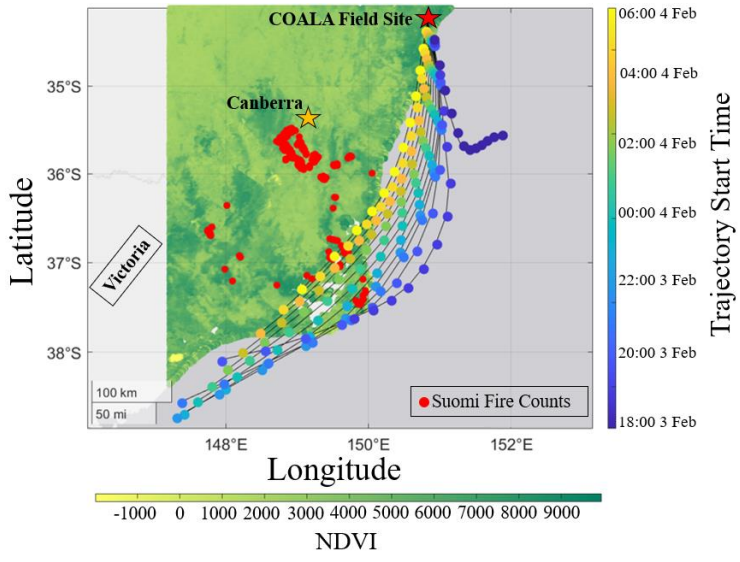

Figure 1: Active fires from 1-5 Feb. 2020 and their proximity to the COALA field site. NDVI is plotted at 250m resolution from the MOD13A1 dataset acquired by measurements via the MODIS Terra satellite. Pixels have been filtered to contain cloud coverage less than 30% and VI Usefulness bits indicating top two tiers of data quality. Fire counts are plotted using the VNP14IMGTDL_NRT data from Suomi VIIRS satellite imaging overlaid with HYSPLIT back trajectories. Each tail represents a trajectory 12 h prior to reaching the site and is colored by its starting time. Circles indicate 1 h intervals moving backwards from the start time.

2.2. PTR-ToF-MS and supporting observations

VOCs were measured using an Ionicon PTR-ToF-MS 4000 which operated with a mass resolution between 2000-3000 FWHM m/Δm and at a mass range spanning m/z = 18-256. The drift tube was held at a temperature of 70° C, pressure at 2.60 mbar, and an E/N = 120 Td (electric field to molecular number density ratio). The instrument was housed in a climate-controlled unit, connected to a 15 m long, 1/4" OD PTFE insulated line attached to a 10 m tall mast, placing inlet height 0.5 m above canopy height. An assist pump was attached pulling an additional 3 SLPM for a residence time of 2.5 s. Peak separation of 1 min averaged spectra was conducted in Ionicon's PTR-Viewer 3 software.

Calibrations were performed using two VOC cylinders designed by Airgas on 31 Jan 2020, three days before measuring the smoke event discussed here. The cylinders contained 17 compounds spanning a mass range of 33-154 Da and are shown in Table S1. Many of these compounds are reported in the final EFs list – methanol, acetonitrile, acetaldehyde, acrolein, acetone, MVK+MACR, benzene, C8-aromatics, and C9-benzenes. All compounds used either do not fragment under these drift tube conditions or have known fragmentary peaks. Instrument zeros were determined using ultra-zero air. Limits of detection (3σ) for calibrated species are also given in Table S1 and range between 5-165 ppt. The raw counts per second (cps) were corrected for instrument transmission, which was determined using a subset of the species in the calibration standards. Corrected cps are then normalized to the reagent ion signal (H_3O^+ ccps x 10^6, ncps) using the methodology described by Sekimoto et al. (2017). For compounds of interest not included in the calibration standards, we use the method described by Sekimoto et al. (2017), which yields uncertainties between 50-100%.

In addition to the PTR-ToF-MS measurements, we use observations of CO, CO_2, and CH_4 obtained from the collocated FTIR system. Information of this instrument and its setup is provided in Griffith et al. (2012).

https://doi.org/10.5194/acp-2021-742
Preprint. Discussion started: 9 September 2021

Atmospheric Chemistry and Physics Discussions

3. Observed CO, VOC, and OVOC Enhancements

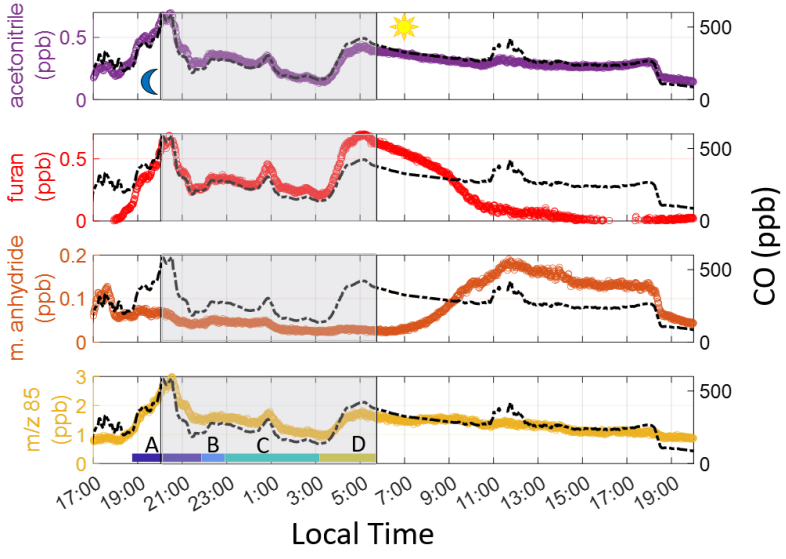

Figure 2: VOCs and CO on 3 – 4 Feb 2020 with the shaded area representing sunset to sunrise. The peak in CO after sunset (start of gray-shaded area) is used to denote the beginning of the smoke event. We limit our analysis to sunrise on the following day. The color labels A-D indicate individual times used to calculate ERs (see section 5.2 in main text).

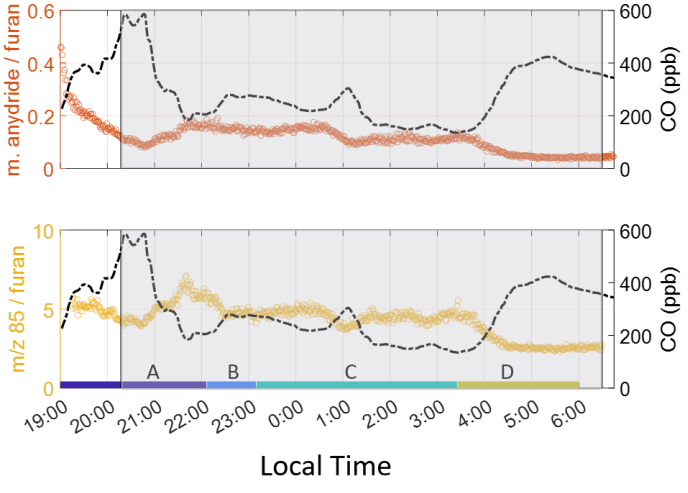

Figure 3: Product-to-reactant ratio for furan oxidation products. Both ratios indicate the period just before sunrise is least oxidized. Again, the color labels A-D indicate individual times used to calculate ERs.

Fig. 2 shows the observations of CO and VOCs during a smoky period on 3 – 4 Feb 2020. CO and acetonitrile – long-lived tracers associated with wildfires (Coggon et al., 2016) – are used to identify the total period of time during which observations were impacted by smoke. Enhancements in both species start at 17:30 local time on 3 Feb and lasting until 19:00 on 4 Feb, when wind direction shifted.

https://doi.org/10.5194/acp-2021-742
Preprint. Discussion started: 9 September 2021

Atmospheric Chemistry and Physics Discussions

We use furan, a short-lived smoke tracer, and its oxidation products to determine which periods of the smoke event represent the least oxidized plume. Furan is highly reactive with OH ($k_{OH + furan}$ = at 4.04 x 10^{-11} cm^3 $molec^{-1}$ s^{-1} 298 K and 1 atm) and NO_3 ($k_{NO3 + furan}$ = at 1.36 x 10^{-12} cm^3 $molec^{-1}$ s^{-1} at 298 K and 1 atm). OH-initiated oxidation produces maleic anhydride, which has low reactivity with both OH and NO_3 (τ_{OH} = 3.99 days, τ_{NO3} = 1.42 days with $[OH]_{Avg}$ = 2 x 10^6 molec cm^{-3} and $[NO_3]_{Avg}$ = 8 x 10^7 molec cm^{-3}, with reaction rate constants from Grosjean (1992) and Bierbach (1994) and no reported direct emissions. The ratio of maleic anhydride-to-furan therefore provides a relative measure of the plume photochemical age. Using aircraft-based observations of wildfire plumes in the Western US, Gkatzelis et al. (2020) found that maleic anhydride-to-furan ratios below 0.10 indicate the plume has undergone little OH processing.

Nighttime in-plume furan oxidation is dominated by NO_3, with contributions from O_3 (Decker et al., 2019). While many BBVOCs are highly reactive with NO_3, there is substantially less research on indicators of NO_3 oxidation. Decker et al. (2019) track NO_3 chemistry using the ratio of total reactive nitrogen (NO_y) to NO_x, and Kodros et al. (2020) examine NO_3-reacted products such as nitrocatechol and nitrophenol of phenolic compounds (e.g. phenol, catechol, cresol). Measurements of NO_y were not made during this field campaign, and NO_3-products of phenols were subject to high uncertainty due to fragmentation in our PTR-ToF-MS measurement. We therefore examine a new indicator of NO_3 processing using furan's dominant NO_3 products – cis-2-butenediol and furanone (Berndt et al., 1997). Both products are relatively long lived, with lifetimes estimated at $\tau_{cis\text{-}2\text{-}butenediol}$=9 days and $\tau_{furanone}$= 8 h assuming an average concentration of $[NO_3]$ = 8 x 10^7 molec cm^{-3} (O'dell et al., 2020). Lab based studies and field campaigns conducted in the US and Australia suggest that furan and furanone EFs are comparable, with study-averaged values for furan ranging from 0.132 – 0.51 g kg^{-1} and 0.27 – 0.57 for furanone (Andreae and Merlet, 2001; Akagi et al., 2011; Hatch et al., 2015; Stockwell et al., 2015; Liu et al., 2017; Koss et al., 2018; Selimovic et al., 2018). No furan EFs have been reported for Australian temperate forests and only one furanone EF is reported from Lawson et al. (2015) at a comparable value at 0.57 g kg^{-1}. Additionally, emissions modeled in Decker et al. (2019) from wildfires suggest that furan and furanone are emitted in roughly equal proportions. As such, we operate not on the assumption of negligible OVOC emissions, but that variability in OVOC/VOC ratios are driven by chemical aging.

Fig. 2 shows furan enhancements, which begin later on Feb 3 than acetonitrile enhancements. Maleic anhydride concentrations are high during the initial period of the smoke event, suggesting significant OH-initiated processing throughout the day before the plume reached the site. After sunrise, furan decays faster than CO, and maleic anhydride concentrations begin to rise, again showing the impact of OH-initiated oxidation. Cis-2-butenediol and furanone are both measured at m/z 85. Enhancements in m/z 85 are seen when the smoke arrives and vary throughout the night. Just prior to sunrise (04:00 – 06:15, local time), both OVOC/VOC ratios rapidly decrease (Fig. 3), corresponding with a rise in furan, CO, and acetonitrile. Maleic anhydride/furan drops to 0.05, which is within the lower range of the chemically younger plumes reported by Gkatzelis et al. (2020). The ratio of m/z 85 to furan is around 2.5. While we cannot use this to quantify plume age since the two products are measured as a sum, we note that this period constitutes the lowest ratio throughout the event, with surrounding periods having ratios 1.6 – 2.8 times greater. We note that at a value of 2.5, this plume has likely undergone significant aging, despite this being the freshest smoke detected during the campaign.

The rapid decreases in OVOC/VOC ratios are unlikely to result from shifts in chemistry alone. Instead, this suggests a shift in meteorological conditions which brings in smoke from a closer source, in agreement with measured wind direction, which shift from northeast to north at this time. We further investigate plume transport using a back-trajectory model.

4. Plume Origin and Transport Time

https://doi.org/10.5194/acp-2021-742
Preprint. Discussion started: 9 September 2021


Atmospheric Chemistry and Physics Discussions

We use a HYSPLIT back-trajectory model (Stein, 2015) to determine the origin and transport time of the smoke arriving at the site throughout the smoke event. The meteorological input used is the Global Data Assimilation (GDAS) dataset. The model was set to assess trajectories at three different altitudes at 10 m, 500 m, and 1500 m above ground level (agl) to capture plume height. Our period of interest spans from 17:00 Feb 3, just before CO enhancements are seen at the site, to 06:00 4 Feb when furan concentrations rapidly decrease. The model was set to calculate a new 12 h trajectory every hour during this time. Back trajectories are shown in Fig. 1. For every hour in the event (each represented by a color), one can track the origin of the sampled airmass 12 h in advance of its arrival.

A shift in trajectories occurred between 17:00 and 18:00 3 Feb, corresponding with the arrival of the smoke plume as indicated by observed CO enhancements. Subsequent trajectories originate near the fires located ~230-375 km from the field site on the southeast coast. The model shows that air masses initially kept at low altitude and were lofted to ~560 m agl when passing over the active fires ~25 km to the south, near Canberra (Fig. S1). The plume descended to 10 m agl as it reached the coast. The model suggests smoke sampled later in the evening (between 04:00 – 06:00 4 Feb) spent more time over land compared to previous points in the event. This shift in trajectories and the increasing intensity of fires near Canberra during this time likely contributed to the decrease in OVOC to VOC age marker ratios. Over the entire course of the event, HYSPLIT analysis suggests transport time from the fires to the field site is around 8 h (>200 km), but potentially shorter for the time frame immediately prior to sunrise (5-8 h, 25 km).

5. Deriving and Contextualizing ER and EFs

5.1 Species selection

To identify compounds which would be suitable for EF derivation, we compare the list of measured ions with compounds identified in previous literature such as Brilli et al. (2014), Hatch et al. (2015), Gilman et al. (2015), Stockwell et al. (2015), Bruns et al. (2017), Koss et al. (2018), and the PTR Library (Pagonis et al., 2019). To corroborate species assignment, we examine correlations of identifiable compounds with CO, acetonitrile, furans, and phenolic compounds which are well-established smoke tracers. We also examine tracer-tracer relationships, for instance the anti-trend between maleic anhydride and furan resulting from OH oxidation. We exclude compounds with low proton affinities that are known to have humidity-dependent calibration factors (e.g., HCHO, HCN). This results in 150 identified VOCs species measured and identified during the smoke event.

We further filter our VOC list by two criteria. First, VOC + NO_3 reaction rates must be included either in the NIST Chemical Kinetics Database (Manion, 2015) or Master Chemical Mechanism (v3.3.1) (Bloss et al., 2005; Jenkin, 1997; Jenkin et al., 2003; Saunders et al., 2003). Second, the VOC must have a significantly long lifetime against NO_3 oxidation to be minimally impacted over the 8 h transit time from the active fires to the field site ($\tau_{BBVOC+NO3}$<8 h, again assuming [NO_3] = 8 x 10^7 molec cm^{-3}). This limits subsequent analysis to 21 long-lived VOCs.

5.2 Calculating Emission Ratios

An ER is defined here as the slope of a linear regression of a given VOC to CO (both in units of ppb). Following Guérette et al. (2018), ERs are reported if correlation between a given VOC and CO are well correlated, with $R^2 \geq 0.5$. High correlation minimizes the impact of the choice of regression method (e.g. orthogonal, York) on calculated slopes (Wu and Yu, 2018). We use a standard linear regression with no error weighting, noting that measurement uncertainty is substantially lower than natural variability.

We first derive ERs using all data from the "freshest" portion of the plume as determined from OVOC/VOC ratios (Marked "D" in Fig. 2). This produces 17 ERs that meet our criteria. We expect this period to provide the most accurate representation of original

https://doi.org/10.5194/acp-2021-742
Preprint. Discussion started: 9 September 2021

Atmospheric Chemistry and Physics Discussions

VOC emissions. We then calculate ERs for more aged portions of the smoke event (Periods A-C, Fig. 2), performing regression analysis on the chemically distinct time periods. The start and end time of each period is determined by visual inspection of VOC/CO behaviors, which all exhibit similar distinct periods. Fig. 4 provides an example of the analysis using acrolein. We average the slopes from each of these lines to derive an average ER for the full smoke event and compare to just the freshest portion of the plume (Period D). We find the using only the freshest smoke compared to using all the data generates very similar results for 14 of the 17 compounds. Relative differences of the resultant ERs are within 1.5 – 47 % with three outliers: butenes (302 %), C8-aromatics (88%), and C3-benzenes (212 %). Five compounds have only 1 ER from all 4 periods (acetylene, pentene, maleic anhydride, benzaldehyde, methyl guaiacol) so there is no standard deviation, but the remaining 12 compounds from period D are captured within 1σ of ERs from periods A-D (shown in Fig. S2). Good agreement between methods allows us to extend our analysis beyond the freshest part of the plume, and therefore allows us to report ERs for a larger number of compounds. When focusing only on the freshest part of the plume, ethyne, pentene, maleic anhydride, and benzaldehyde must be excluded due to insufficient R^2 with CO. All ERs reported here and used in EF calculation use the "average over evening" method and include these compounds. Additionally, only one ER for CO_2 and CH_4 have been calculated using the dataset from periods A-D. Both these compounds are long-lived, and from visual inspection, they do not form distinct time periods like the VOC ERs (shown in Fig. 4).

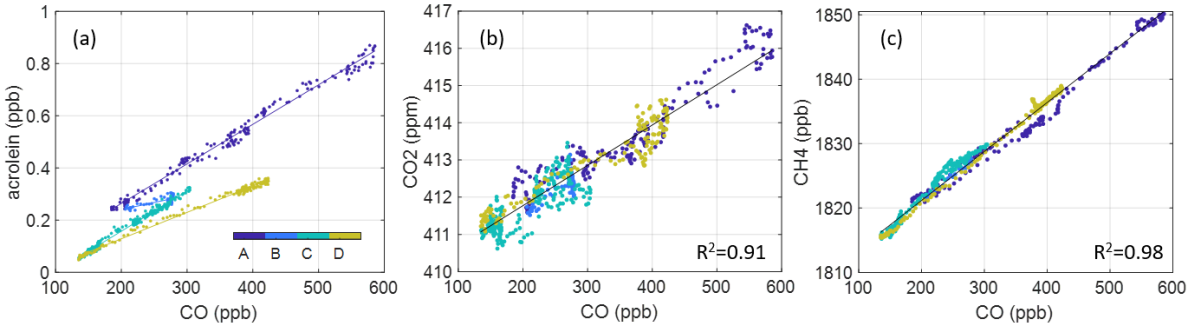

Figure 4: Example ER analysis (a) using acrolein, wherein the smoke event is partitioned into 4 periods over the evening. Average ERs (slopes) from periods A-C agree closely with those in the freshest portion of the plume (D). Panels (b) and (c) show the singular ERs derived for CO_2 and CH_4 using the entire nighttime dataset (A-D).

5.3 Calculating Emission Factors

Emission factors are defined as the mass of some trace gas emitted per mass of dry biomass burnt. The most direct way of calculating this quantity is capturing total emissions released from a fire as well as knowing the quantity of fuel burnt. Unless experiments are conducted in a laboratory setting, these quantities are not known. As such, emission factors are calculated according to the carbon mass balance method (Akagi et al., 2011; Selimovic et al., 2018), using CO as the reference gas for the 21 reported species which produces the following equation:

$$EF_X = F_{carbon} \times 1000 \times MM_x/MM_C \times ER_{X/CO} / \sum ER_{Y/CO} \quad (1)$$

https://doi.org/10.5194/acp-2021-742
Preprint. Discussion started: 9 September 2021

Atmospheric Chemistry and Physics Discussions

where F_{carbon}=0.5 and is the assumed carbon fractional content of the fuel as used in previous studies (Akagi et al., 2011; Paton-Walsh et al., 2014). MM_X is the molar mass of compound X, MM_C is the molar mass of carbon, $ER_{X/CO}$ is the CO ER of X, and $\sum ER_{Y/CO}$ is the sum of $ER_{CO2/CO}$, $ER_{CH4/CO}$, and $ER_{CO/CO}$. These ERs constitute the major volatilized carbon components of the plume, but the resulting EFs may be overestimated by 1-2% (Andreae and Merlet, 2001) as this method assumes all volatilized carbon is detected including particulate carbon, VOCs, CO, and CO_2.

EFs derived in this work are presented in Table 1 alongside results from 2 eastern Australia-based studies by Lawson et al. (2015) and Guérette et al. (2018), 2 western US-based studies sampling emissions from corresponding temperate fuel types by Liu et al. (2017) and Permar et al. (2021), and 1 study by (Akagi et al., 2011) that provides EFs for general temperate zones.

Table 1: EFs (g kg^{-1}) derived in this work compared to 2 studies conducted in the same or near temperate Australian forests, 2 US-based aircraft campaigns sampling western temperate US fuels, and 1 study reporting EFs across geographically distant temperate forests.*

		Biome Location					
		AU	AU	AU	US	US	Temperate Forests
Compound	Formula	This Work	Guerette et al. (2018)	Lawson et al. (2015)	Liu et al. (2017)	Permar et al. (2021)	Akagi et al. (2011)
Ethyne	C_2H_2	0.20 ± —	0.35 ± 0.09	—	0.24 ± 0.04	0.21 ± 0.17	0.29 ± 0.10
Methanol	CH_4O	1.99 ± 0.56	3.0 ± 0.5	2.07 ± —	2.45 ± 1.43	1.50 ± 0.39	1.93 ± 1.38
Acetonitrile	C_2H_3N	0.16 ± 0.03	0.70 ± 0.10	0.25 ± —	0.25 ± 0.13	0.31 ± 0.15	—
Propene	C_3H_6	0.19 ± 0.04	—	—	0.35 ± 0.01	0.74 ± 0.62	0.95 ± 0.54
Acetaldehyde	C_2H_4O	0.55 ± 0.20	1.20 ± 0.30	0.92 ± —	1.64 ± 0.52	1.70 ± 0.43	—
Acrolein	C_3H_4O	0.23 ± 0.09	—	—	— *	0.40 ± 0.18	—
Butenes	C_4H_8	0.14 ± 0.14	—	—	0.14 ± 0.01	0.26 ± 0.12	—
Acetone	C_3H_6O	0.52 ± 0.26	0.80 ± 0.20	0.54 ± —	1.13 ± 0.82	0.84 ± 0.22	—
MVK+MACR	C_4H_6O	0.17 ± 0.04	1.0 ± 0.30	0.38 ± —	0.33 ± 0.06	0.39 ± 0.15	—
Pentene	C_5H_{10}	0.10 ± —	—	—	0.26 ± 0.005	0.015 ± 0.0084	—
Benzene	C_6H_6	0.24 ± 0.09	0.39 ± 0.07	0.69 ± —	0.43 ± 0.12	0.50 ± 0.14	—
Furanone	$C_4H_4O_2$	0.88 ± 0.34	—	0.57 ± —	0.39 ± —	0.32 ± 0.11	—
Pentanones	$C_5H_{10}O$	0.05 ± 0.01	—	—	—	0.062 ± 0.023	—
Methyl-propanoate	$C_4H_8O_2$	0.07 ± 0.03	—	—	—	0.081 ± 0.036	—
Maleic-anhydride	$C_4H_2O_3$	0.06 ± —	—	—	—	0.14 ± 0.072	—
Methyl-methacrylate	$C_5H_8O_2$	0.43 ± 0.25	—	—	—	0.11 ± 0.045	—
Benzaldehyde	C_7H_6O	0.05 ± —	—	—	—	0.04 ± 0.026	—
C8-aromatics	C_8H_{10}	0.07 ± 0.04	0.11 ± 0.03	0.26 ± —	0.15 ± 0.004	0.21 ± 0.08	—
C3-benzene	C_9H_{12}	0.06 ± 0.06	—	0.27 ± —	—	0.069 ± 0.031	—
Methylbenzoic-acid	$C_8H_8O_2$	0.01 ± 0.001	—	—	—	0.066 ± 0.029	—
Methyl guaiacol	$C_8H_{10}O_2$	0.04 ± —	—	—	—	0.14 ± 0.11	—

* Dashes indicate either EF or EF variability not reported in study.

First, in comparison with the Australia-based studies, Guérette et al. (2018) reports EFs notably larger than those presented in this work, with only benzene and C8-aromatics showing good agreement. Except for these two compounds and C3-benzenes, Guérette et al. (2018) reports larger EFs than Lawson et al. (2015) and none within agreement. Our results more closely agree with Lawson

https://doi.org/10.5194/acp-2021-742
Preprint. Discussion started: 9 September 2021


Atmospheric Chemistry and Physics Discussions

et al (2015) with methanol, acetone, and furanone EFs within 1σ, and acetonitrile and acetaldehyde falling within a factor of 2. This agreement is likely due to both this work and Lawson et al. (2015) examining opportunistically intercepted smoke plumes that experienced some processing whereas Guérette et al. (2018) sampled near-source, controlled ground burns. Guérette et al. (2018) reports an acetonitrile EF ~4.5 times higher than this work and ~3 times greater than Lawson et al. (2015) constituting one of the largest disparities. This is attributed to the native and abundant Acacias which are N-fixing species located mainly in forest understories. Their measurements likely had a higher proportion of this foliage constituting the total fuel load due to both proximity to the forest floor and resulting leaf litter. Another of the largest differences is MVK+MACR, which shows a disparity of ~6 times this work and 3 times that of Lawson et al. (2015). This is also most likely explained by differences in sampling approach in that proportional contributions of vegetation vary and plumes in Guérette et al. (2018) did not undergo any dilution or photochemical processing.

In comparison with US-based studies, ethyne, methanol, acetonitrile, butenes, acetone, and benzene agree across both studies within 1σ, with acrolein, pentanone, methyl propanoate, C3-benzenes, and methyl guaiacol agreeing very well with values reported by Permar et al. (2021). It should be noted that though within the estimated uncertainties, the value for methyl guaiacol reported by Permar et al. (2021) is ~3.5 times greater than the value in this work, which constitutes another of the largest disparities in this dataset. Additionally, ethyne and methanol agree well with values from Akagi et al. (2011). However, propene is on the range of ~3 – 4 times less than values from Akagi et al. (2011) and Permar et al. (2021), and while within a factor of 2 is outside of any variability in (Liu et al., 2017). Pentene is not within agreement of either US-based study as both have small corresponding variabilities (between 1 – 5 %), and additionally is ~2.5 times less than the value in (Liu et al., 2017). This could result from differing fuel types. The EF for furanone in this work is also expectedly larger than both other values presented here at ~3 times greater than Permar et al. (2021). This is due to the plume sampled in this work undergoing the longest transport of any plumes measured in other studies.

Perhaps an unexpected finding is that EFs derived in this work agree better with observations in the US than the Guerette et al. (2018) study, which was in the same region as the COALA measurements. It should be noted that all studies except Guerette et al. (2018) are from plumes sampled several km downwind. Differences previously characterized as arising from varying fuel types may actually result from measurement approaches to deriving EFs and proximity to emission source. Agreement across results from this work and from the US-based studies lends credence to the use of newly presented EFs for modeling purposes in temperate Australian forests.

6. Conclusions

EFs were derived for a total of 21 trace gas species via measurements from a PTR-ToF-MS and an FTIR spectrometer. The COALA ground-based field campaign opportunistically sampled a sustained biomass burning plume from 3 – 4 Feb 2020 during the 2019-2020 wildfire season in New South Wales, Australia. We determined via HYSPLIT trajectories that the most likely pathway traveled by the plume was from a distance ranging from ~230-375 km south from fires along the temperate forests of the east coast with contributions from more inland fires near Canberra, Australia. This plume lofted to an altitude of 500 m agl as it passed over active fires ~8 h out from the field site, before descending down to 10 m agl while traveling over the ocean, and reaching the site at 17:30 local time. All data used in the derivation of EFs was limited from sunset on 3 Feb to sunrise on 4 Feb as this period showed the greatest enhancements of reactive BB tracers like furan. Through visual inspection, we partitioned this plume event into 4 portions, and calculated and averaged the individual ERs. We used two age marker ratios derived from furan radical oxidation to determine the freshest portion of the plume and found that ERs from this portion corresponded well with the averaged ERs

https://doi.org/10.5194/acp-2021-742
Preprint. Discussion started: 9 September 2021


Atmospheric Chemistry and Physics Discussions

(within 1σ). Using EFs from the entire evening allowed for the inclusion of three more VOC EFs into this analysis which, for the freshest portion of the plume, did not meet the selection criteria for ERs.

We have further characterized wildfire emissions in Australia's temperate region by providing a more comprehensive suite of VOC EFs. This suite introduces new EFs for acrolein, pentanones/methylbutanal, methyl propanoate, methyl methacrylate, pentene, maleic anhydride, benzaldehyde, methyl guaiacol, and methylbenzoic acid. When compared with values reported from 2 Australian studies located in the same or nearby temperate forests, we find mixed agreement with results from Guérette et al. (2018) as only two values are captured within our EF variability, with acetonitrile differing by a factor of ~4.5 times and MVK+MACR differing by ~6 times. However, 2 compounds are within the range of variability for Lawson et al. (2015) and 2 others are well within a factor of 2, which indicates decent agreement. Furthermore, comparison with two recent US studies that report data on analogous temperate zones, as well as one report covering global temperate regions, show generally good agreement for 11 of the 21 compounds, with several others within a factor of 2. This closer agreement with these studies, as well as that of Lawson et al. (2015), is likely due to the measurement approach when deriving EFs as both US-based studies were aircraft campaigns, and the Australia-based study intercepted a transported plume much like this work. Guérette et al. (2018) sampled controlled burns on a ground campaign virtually at the emission source. This indicates that variability previously ascribed to differing fuel types may be overshadowed by sampling approach and that comprehensive measurements from US-based studies may be useful for studying Australian biomes. Agreement with both Lawson et al. (2015) and the US-based studies indicates that results here are valid for future use in Australian, biome-specific biomass burning studies. Chemically comprehensive near-source observations of Australian fuel types are needed to evaluate the importance delineating temperate forest EFs in different regions across the globe.

Data Availability. Data are available from PANGAEA archive at https://doi.pangaea.de/10.1594/PANGAEA.927277.

Supplement. The supplement related to this article is available online at:

Author Contributions. Asher P. Mouat conducted PTR-ToF-MS measurements and subsequent data analysis. Jack Simmons, Clare Paton-Walsh, and Jhonathan Ramirez-Gamboa oversaw the maintenance and in-person operation of the PTR-ToF-MS for much of the COALA field campaign. CO measurements were provided by David Griffith. Clare Paton-Walsh led the COALA campaign, whilst Jennifer Kaiser led PTR-ToF-MS instrument deployment and data analysis. All coauthors have provided substantial input during the process of drafting this work.

Competing interests. The authors declare that they have no conflict of interest.

Acknowledgements. This work was supported by NSF grant GR00003303. We thank Travis Naylor, Ian Galbally and all the UOW COALA team for their aid in conducting measurements during the field campaign and all input thereafter. We additionally gratefully acknowledge the NOAA Air Resources Laboratory (ARL) for providing the HYSPLIT transport and dispersion model used for analysis in this publication. We acknowledge the use of data and/or imagery from NASA's Land, Atmosphere Near real-time Capability for EOS (LANCE) system (*https://earthdata.nasa.gov/lance*), part of NASA's Earth Observing System Data and Information System (EOSDIS).

References

https://doi.org/10.5194/acp-2021-742
Preprint. Discussion started: 9 September 2021

Akagi, S. K., Yokelson, R. J., Wiedinmyer, C., Alvarado, M. J., Reid, J. S., Karl, T., Crounse, J. D., and Wennberg, P. O.: Emission factors for open and domestic biomass burning for use in atmospheric models, Atmos. Chem. Phys., 11, 4039-4072, 10.5194/acp-11-4039-2011, 2011.

Akagi, S. K., Craven, J. S., Taylor, J. W., McMeeking, G. R., Yokelson, R. J., Burling, I. R., Urbanski, S. P., Wold, C. E., Seinfeld, J. H., Coe, H., Alvarado, M. J., and Weise, D. R.: Evolution of trace gases and particles emitted by a chaparral fire in California, Atmos. Chem. Phys., 12, 1397-1421, 10.5194/acp-12-1397-2012, 2012.

Akagi, S. K., Yokelson, R. J., Burling, I. R., Meinardi, S., Simpson, I., Blake, D. R., McMeeking, G. R., Sullivan, A., Lee, T., Kreidenweis, S., Urbanski, S., Reardon, J., Griffith, D. W. T., Johnson, T. J., and Weise, D. R.: Measurements of reactive trace gases and variable O₃ formation rates in some South Carolina biomass burning plumes, Atmos. Chem. Phys., 13, 1141-1165, 10.5194/acp-13-1141-2013, 2013.

Andreae, M. O. and Merlet, P.: Emission of trace gases and aerosols from biomass burning, Global Biogeohemical Cycles, 15, 955-966, https://doi.org/10.1029/2000GB001382, 2001.

Berndt, T., Böge, O., and Rolle, W.: Products of the Gas-Phase Reactions of NO3 Radicals with Furan and Tetramethylfuran, Environmental Science & Technology, 31, 1157-1162, 10.1021/es960669z, 1997.

Bierbach, A., Barnes, Ian., Becker, K.H., Wiesen, E.: Atmospheric Chemistry of Unsaturated Carbonyls: Butenedial, 4-Oxo-2-pentenal, 3-Hexene-2,5-dione, Maleic Anhydride, 3/fFuran-2-one, and 5-Methyl-3H-furan-2-one, Environ. Sci. Tech., 28, 715-729, 1994.

Bloss, C., Wagner, V., Jenkin, M. E., Volkamer, R., Bloss, W. J., Lee, J. D., Heard, D. E., Wirtz, K., Martin-Reviejo, M., Rea, G., Wenger, J. C., and Pilling, M. J.: Development of a detailed chemical mechanism (MCMv3.1) for the atmospheric oxidation of aromatic hydrocarbons, Atmos. Chem. Phys., 5, 641-664, 10.5194/acp-5-641-2005, 2005.

Brilli, F., Gioli, B., Ciccioli, P., Zona, D., Loreto, F., Janssens, I. A., and Ceulemans, R.: Proton Transfer Reaction Time-of-Flight Mass Spectrometric (PTR-TOF-MS) determination of volatile organic compounds (VOCs) emitted from a biomass fire developed under stable nocturnal conditions, Atmospheric Environment, 97, 54-67, https://doi.org/10.1016/j.atmosenv.2014.08.007, 2014.

Bruns, E. A., Slowik, J. G., El Haddad, I., Kilic, D., Klein, F., Dommen, J., Temime-Roussel, B., Marchand, N., Baltensperger, U., and Prévôt, A. S. H.: Characterization of gas-phase organics using proton transfer reaction time-of-flight mass spectrometry: fresh and aged residential wood combustion emissions, Atmos. Chem. Phys., 17, 705-720, 10.5194/acp-17-705-2017, 2017.

Burling, I. R., Yokelson, R. J., Akagi, S. K., Urbanski, S. P., Wold, C. E., Griffith, D. W. T., Johnson, T. J., Reardon, J., and Weise, D. R.: Airborne and ground-based measurements of the trace gases and particles emitted by prescribed fires in the United States, Atmos. Chem. Phys., 11, 12197-12216, 10.5194/acp-11-12197-2011, 2011.

Coggon, M. M., Veres, P. R., Yuan, B., Koss, A., Warneke, C., Gilman, J. B., Lerner, B. M., Peischl, J., Aikin, K. C., Stockwell, C. E., Hatch, L. E., Ryerson, T. B., Roberts, J. M., Yokelson, R. J., and de Gouw, J. A.: Emissions of nitrogen-containing organic compounds from the burning of herbaceous and arboraceous biomass: Fuel composition dependence and the variability of commonly used nitrile tracers, Geophysical Research Letters, 43, 9903-9912, https://doi.org/10.1002/2016GL070562, 2016.

de Gouw, J. A., Warneke, C., Stohl, A., Wollny, A. G., Brock, C. A., Cooper, O. R., Holloway, J. S., Trainer, M., Fehsenfeld, F. C., Atlas, E. L., Donnelly, S. G., Stroud, V., and Lueb, A.: Volatile organic compounds composition of merged and aged forest fire plumes from Alaska and western Canada, Journal of Geophysical Research: Atmospheres, 111, https://doi.org/10.1029/2005JD006175, 2006.

Decker, Z. C. J., Zarzana, K. J., Coggon, M., Min, K.-E., Pollack, I., Ryerson, T. B., Peischl, J., Edwards, P., Dubé, W. P., Markovic, M. Z., Roberts, J. M., Veres, P. R., Graus, M., Warneke, C., de Gouw, J., Hatch, L. E., Barsanti, K. C., and Brown, S. S.: Nighttime Chemical Transformation in Biomass Burning Plumes: A Box Model Analysis Initialized with Aircraft Observations, Environmental Science & Technology, 53, 2529-2538, 10.1021/acs.est.8b05359, 2019.

Didan, K.: MODIS/Terra Vegetation Indices 16-Day L3 Global 250m SIN Grid V061 [dataset], https://doi.org/10.5067/MODIS/MOD13Q1.061, 2021.

Filkov, A. I., Ngo, T., Matthews, S., Telfer, S., and Penman, T. D.: Impact of Australia's catastrophic 2019/20 bushfire season on communities and environment. Retrospective analysis and current trends, Journal of Safety Science and Resilience, 1, 44-56, https://doi.org/10.1016/j.jnlssr.2020.06.009, 2020.

Gilman, J. B., Lerner, B. M., Kuster, W. C., Goldan, P. D., Warneke, C., Veres, P. R., Roberts, J. M., de Gouw, J. A., Burling, I. R., and Yokelson, R. J.: Biomass burning emissions and potential air quality impacts of volatile organic compounds and other trace gases from fuels common in the US, Atmos. Chem. Phys., 15, 13915-13938, 10.5194/acp-15-13915-2015, 2015.

Gkatzelis, G., Coggon, M. M., Sekimoto, K., Gilman, J., Lamplugh, A., Bourgeois, I., Peischl, J., Ryerson, T. B., Veres, P. R., Neuman, J. A., Womack, C., Brown, S. S., Rollins, A. W., Rickly, P., Bela, M., Schwantes, R., Katich, J. M., Lindaas, J., Jimenez, J. L., Campuzano Jost, P., Guo, H., Nault, B. A., Pagonis, D., Schueneman, M., Day, D. A., Wisthaler, A., Piel, F., Tomsche, L., Mikoviny, T., Hair, J. W., Shingler, T. J., Fenn, M. A., Selimovic, V., Huey, L. G., Ji, Y., Lee, Y. R., Tanner, D., Nowak, J. B., DiGangi, J. P., Halliday, H. S., Diskin, G. S., Fried, A., Weibring, P., Wolfe, G. M., St Clair, J. M., Hannun, R. A., Liao, J., Hanisco, T. F., Travis, K., Roberts, J., Trainer, M., Schwarz, J. P., Crawford, J. H., and Warneke, C.: Non-methane organic and nitrogen emissions from wildfire plumes during FIREX-AQ, AGU Fall Meeting, Online, December 01, 20202020.

Gregory, R. W., Yayne-abeba, A., Matthew, S. L., and Yu-Mei, H.: Impacts of a large boreal wildfire on ground level atmospheric concentrations of PAHs, VOCs and ozone, Atmospheric Environment, 178, 19-30, https://doi.org/10.1016/j.atmosenv.2018.01.013, 2018.

https://doi.org/10.5194/acp-2021-742
Preprint. Discussion started: 9 September 2021

Atmospheric Chemistry and Physics Discussions

Griffith, D. W. T., Deutscher, N. M., Caldow, C., Kettlewell, G., Riggenbach, M., and Hammer, S.: A Fourier transform infrared trace gas and isotope analyser for atmospheric applications, Atmos. Meas. Tech., 5, 2481-2498, 10.5194/amt-5-2481-2012, 2012.

Grosjean, D., Williams, E.L.: Environmental persistence of organic compounds estimated from structure-reactivity and linear free-energy relationships. Unsaturated aliphatics, Atmospheric Environment. Part A. General Topics, 26, 1395-1405, https://doi.org/10.1016/0960-1686(92)90124-4, 1992.

Guérette, E. A., Paton-Walsh, C., Desservettaz, M., Smith, T. E. L., Volkova, L., Weston, C. J., and Meyer, C. P.: Emissions of trace gases from Australian temperate forest fires: emission factors and dependence on modified combustion efficiency, Atmos. Chem. Phys., 18, 3717-3735, 10.5194/acp-18-3717-2018, 2018.

Hatch, L. E., Luo, W., Pankow, J. F., Yokelson, R. J., Stockwell, C. E., and Barsanti, K. C.: Identification and quantification of gaseous organic compounds emitted from biomass burning using two-dimensional gas chromatography–time-of-flight mass spectrometry, Atmos. Chem. Phys., 15, 1865-1899, 10.5194/acp-15-1865-2015, 2015.

Hatch, L. E., Yokelson, R. J., Stockwell, C. E., Veres, P. R., Simpson, I. J., Blake, D. R., Orlando, J. J., and Barsanti, K. C.: Multi-instrument comparison and compilation of non-methane organic gas emissions from biomass burning and implications for smoke-derived secondary organic aerosol precursors, Atmos. Chem. Phys., 17, 1471-1489, 10.5194/acp-17-1471-2017, 2017.

Ito, A. and Penner, J. E.: Global estimates of biomass burning emissions based on satellite imagery for the year 2000, Journal of Geophysical Research: Atmospheres, 109, https://doi.org/10.1029/2003JD004423, 2004.

Jenkin, M. E., Saunders, S. M., Wagner, V., and Pilling, M. J.: Protocol for the development of the Master Chemical Mechanism, MCM v3 (Part B): tropospheric degradation of aromatic volatile organic compounds, Atmos. Chem. Phys., 3, 181-193, 10.5194/acp-3-181-2003, 2003.

Jenkin, M. E., Saunders, S.M., and Pilling, Michael, J.: The tropospheric degradation of volatile organic compounds: a protocol for mechanism development, Atmospheric Environment, 31, 81-104, https://doi.org/10.1016/S1352-2310(96)00105-7, 1997.

Keywood, M., Kanakidou, M., Stohl, A., Dentener, F., Grassi, G., Meyer, C. P., Torseth, K., Edwards, D., Thompson, A. M., Lohmann, U., and Burrows, J.: Fire in the Air: Biomass Burning Impacts in a Changing Climate, Critical Reviews in Environmental Science and Technology, 43, 40-83, 10.1080/10643389.2011.604248, 2013.

Kodros, J. K., Papanastasiou, D. K., Paglione, M., Masiol, M., Squizzato, S., Florou, K., Skyllakou, K., Kaltsonoudis, C., Nenes, A., and Pandis, S. N.: Rapid dark aging of biomass burning as an overlooked source of oxidized organic aerosol, Proceedings of the National Academy of Sciences, 117, 33028, 10.1073/pnas.2010365117, 2020.

Koss, A. R., Sekimoto, K., Gilman, J. B., Selimovic, V., Coggon, M. M., Zarzana, K. J., Yuan, B., Lerner, B. M., Brown, S. S., Jimenez, J. L., Krechmer, J., Roberts, J. M., Warneke, C., Yokelson, R. J., and de Gouw, J.: Non-methane organic gas emissions from biomass burning: identification, quantification, and emission factors from PTR-ToF during the FIREX 2016 laboratory experiment, Atmos. Chem. Phys., 18, 3299-3319, 10.5194/acp-18-3299-2018, 2018.

Lawson, S. J., Keywood, M. D., Galbally, I. E., Gras, J. L., Cainey, J. M., Cope, M. E., Krummel, P. B., Fraser, P. J., Steele, L. P., Bentley, S. T., Meyer, C. P., Ristovski, Z., and Goldstein, A. H.: Biomass burning emissions of trace gases and particles in marine air at Cape Grim, Tasmania, Atmos. Chem. Phys., 15, 13393-13411, 10.5194/acp-15-13393-2015, 2015.

Liu, X., Zhang, Y., Huey, L. G., Yokelson, R. J., Wang, Y., Jimenez, J. L., Campuzano-Jost, P., Beyersdorf, A. J., Blake, D. R., Choi, Y., St. Clair, J. M., Crounse, J. D., Day, D. A., Diskin, G. S., Fried, A., Hall, S. R., Hanisco, T. F., King, L. E., Meinardi, S., Mikoviny, T., Palm, B. B., Peischl, J., Perring, A. E., Pollack, I. B., Ryerson, T. B., Sachse, G., Schwarz, J. P., Simpson, I. J., Tanner, D. J., Thornhill, K. L., Ullmann, K., Weber, R. J., Wennberg, P. O., Wisthaler, A., Wolfe, G. M., and Ziemba, L. D.: Agricultural fires in the southeastern U.S. during SEAC4RS: Emissions of trace gases and particles and evolution of ozone, reactive nitrogen, and organic aerosol, Journal of Geophysical Research: Atmospheres, 121, 7383-7414, https://doi.org/10.1002/2016JD025040, 2016.

Liu, X., Huey, L. G., Yokelson, R. J., Selimovic, V., Simpson, I. J., Müller, M., Jimenez, J. L., Campuzano-Jost, P., Beyersdorf, A. J., Blake, D. R., Butterfield, Z., Choi, Y., Crounse, J. D., Day, D. A., Diskin, G. S., Dubey, M. K., Fortner, E., Hanisco, T. F., Hu, W., King, L. E., Kleinman, L., Meinardi, S., Mikoviny, T., Onasch, T. B., Palm, B. B., Peischl, J., Pollack, I. B., Ryerson, T. B., Sachse, G. W., Sedlacek, A. J., Shilling, J. E., Springston, S., St. Clair, J. M., Tanner, D. J., Teng, A. P., Wennberg, P. O., Wisthaler, A., and Wolfe, G. M.: Airborne measurements of western U.S. wildfire emissions: Comparison with prescribed burning and air quality implications, Journal of Geophysical Research: Atmospheres, 122, 6108-6129, https://doi.org/10.1002/2016JD026315, 2017.

Liu, Y., Stanturf, J., and Goodrick, S.: Trends in global wildfire potential in a changing climate, Forest Ecology and Management, 259, 685-697, https://doi.org/10.1016/j.foreco.2009.09.002, 2010.

Manion, J. A., Huie, R.E., Levin, R.D., Burgess Jr., Orkin, V.L., Tsang, W., McGivern, W.S., Hudgens, J.W., Knyazev, V.D., Atkinson, D.B., Chai., E., Tereza, A.M., Lin, C.Y., Allison, T.C., Mallard, W.G., Westly, F., Herron, J.T., Hampson, R.F., Frizzell, D.H.: NIST Chemical Kinetics Database (2015.09) [dataset], 2015.

O'Dell, K., Hornbrook, R. S., Permar, W., Levin, E. J. T., Garofalo, L. A., Apel, E. C., Blake, N. J., Jarnot, A., Pothier, M. A., Farmer, D. K., Hu, L., Campos, T., Ford, B., Pierce, J. R., and Fischer, E. V.: Hazardous Air Pollutants in Fresh and Aged Western US Wildfire Smoke and Implications for Long-Term Exposure, Environmental Science & Technology, 54, 11838-11847, 10.1021/acs.est.0c04497, 2020.

Pagonis, D., Sekimoto, K., and de Gouw, J.: A Library of Proton-Transfer Reactions of H3O+ Ions Used for Trace Gas Detection, Journal of the American Society for Mass Spectrometry, 30, 1330-1335, 10.1007/s13361-019-02209-3, 2019.

Paton-Walsh, C., Smith, T. E. L., Young, E. L., Griffith, D. W. T., and Guérette, É. A.: New emission factors for Australian vegetation fires measured using open-path Fourier transform infrared spectroscopy – Part 1: Methods and Australian temperate forest fires, Atmos. Chem. Phys., 14, 11313-11333, 10.5194/acp-14-11313-2014, 2014.

Permar, W., Wang, Q., Selimovic, V., Wielgasz, C., Yokelson, R. J., Hornbrook, R. S., Hills, A. J., Apel, E. C., Ku, I.-T., Zhou, Y., Sive, B. C., Sullivan, A. P., Collett Jr, J. L., Campos, T. L., Palm, B. B., Peng, Q., Thornton, J. A., Garofalo, L. A., Farmer, D. K., Kreidenweis, S. M., Levin, E. J. T., DeMott, P. J., Flocke, F., Fischer, E. V., and Hu, L.: Emissions of Trace Organic Gases From Western U.S. Wildfires Based on WE-CAN Aircraft Measurements, Journal of Geophysical Research: Atmospheres, 126, e2020JD033838, https://doi.org/10.1029/2020JD033838, 2021.

Saunders, S. M., Jenkin, M. E., Derwent, R. G., and Pilling, M. J.: Protocol for the development of the Master Chemical Mechanism, MCM v3 (Part A): tropospheric degradation of non-aromatic volatile organic compounds, Atmos. Chem. Phys., 3, 161-180, 10.5194/acp-3-161-2003, 2003.

Sekimoto, K., Li, S.-M., Yuan, B., Koss, A., Coggon, M., Warneke, C., and de Gouw, J.: Calculation of the sensitivity of proton-transfer-reaction mass spectrometry (PTR-MS) for organic trace gases using molecular properties, International Journal of Mass Spectrometry, 421, 71-94, https://doi.org/10.1016/j.ijms.2017.04.006, 2017.

Sekimoto, K., Koss, A. R., Gilman, J. B., Selimovic, V., Coggon, M. M., Zarzana, K. J., Yuan, B., Lerner, B. M., Brown, S. S., Warneke, C., Yokelson, R. J., Roberts, J. M., and de Gouw, J.: High- and low-temperature pyrolysis profiles describe volatile organic compound emissions from western US wildfire fuels, Atmos. Chem. Phys., 18, 9263-9281, 10.5194/acp-18-9263-2018, 2018.

Selimovic, V., Yokelson, R. J., Warneke, C., Roberts, J. M., de Gouw, J., Reardon, J., and Griffith, D. W. T.: Aerosol optical properties and trace gas emissions by PAX and OP-FTIR for laboratory-simulated western US wildfires during FIREX, Atmos. Chem. Phys., 18, 2929-2948, 10.5194/acp-18-2929-2018, 2018.

Stein, A. F., Draxler, R.R., Rolph, G.D., Stunder, B.J.B., Cohen, M.D., Ngan, F.: NOAA's HYSPLIT atmospheric transport and dispersion modeling system, Bull. Amer. Meteor. Soc., 96, 2059-2077, https://doi.org/10.1175/BAMS-D-14-00110.1, 2015.

Stockwell, C. E., Veres, P. R., Williams, J., and Yokelson, R. J.: Characterization of biomass burning emissions from cooking fires, peat, crop residue, and other fuels with high-resolution proton-transfer-reaction time-of-flight mass spectrometry, Atmos. Chem. Phys., 15, 845-865, 10.5194/acp-15-845-2015, 2015.

van der Werf, G. R., Randerson, J. T., Giglio, L., Collatz, G. J., Mu, M., Kasibhatla, P. S., Morton, D. C., DeFries, R. S., Jin, Y., and van Leeuwen, T. T.: Global fire emissions and the contribution of deforestation, savanna, forest, agricultural, and peat fires (1997–2009), Atmos. Chem. Phys., 10, 11707-11735, 10.5194/acp-10-11707-2010, 2010.

Wang, X., Meyer, C. P., Reisen, F., Keywood, M., Thai, P. K., Hawker, D. W., Powell, J., and Mueller, J. F.: Emission Factors for Selected Semivolatile Organic Chemicals from Burning of Tropical Biomass Fuels and Estimation of Annual Australian Emissions, Environmental Science & Technology, 51, 9644-9652, 10.1021/acs.est.7b01392, 2017.

Wu, C. and Yu, J. Z.: Evaluation of linear regression techniques for atmospheric applications: the importance of appropriate weighting, Atmos. Meas. Tech., 11, 1233-1250, 10.5194/amt-11-1233-2018, 2018.